Published in final edited form as:
Nucl Med Biol. 2011 August ; 38(6): 897–906. doi:10.1016/j.nucmedbio.2011.01.009.

Striatal adenosine A_{2A} receptor mediated PET Imaging in 6-hydroxydopamine lesioned rats using [^{18}F]-MRS5425

Abesh Kumar Bhattacharjee[1], **Lixin Lang**[1], **Orit Jacobson**[1], **Bidhan Shinkre**[2], **Ying Ma**[1], **Gang Niu**[1,3], **William C. Trenkle**[2], **Kenneth A. Jacobson**[4], **Xiaoyuan Chen**[1], and **Dale O. Kiesewetter**[1,*]

[1]Laboratory of Molecular Imaging and Nanomedicine, National Institute of Biomedical Imaging and Bioengineering, National Institutes of Health, Bethesda, MD, 20892

[2]Chemical Biology Unit, Laboratory of Cell Biochemistry & Biology, National Institute of Diabetes & Digestive & Kidney Diseases, National Institutes of Health, Bethesda, MD, 20892

[3]Department of Radiology and Imaging Sciences, Warren Grant Magnuson Clinical Center, National Institutes of Health, Bethesda, MD, 20892

[4]Molecular Recognition Section, Laboratory of Bioorganic Chemistry, National Institute of Diabetes & Digestive & Kidney Diseases, National Institutes of Health, Bethesda, MD, 20892

Abstract

Introduction—A_{2A} receptors are expressed in the basal ganglia, specifically in striatopallidal GABAergic neurons in the striatum (caudate-putamen). This brain region undergoes degeneration of pre-synaptic dopamine projections and depletion of dopamine in Parkinson's disease. We developed a^{18}F-labeled A_{2A} analog radiotracer ([^{18}F]-**MRS5425**) for A_{2A} receptor imaging using positron emission tomography (PET). We hypothesized that this tracer could image A_{2A} receptor changes in the rat model for Parkinson disease, which is created following unilateral injection of the monoaminergic toxin, 6-hydroxydopamine (6-OHDA) into the substantia nigra.

Methods—[^{18}F]-**MRS5425** was injected intravenously in anesthetized rats and PET imaging data collected. Image derived percent injected doses per gram (%ID/g) in regions of interest (ROIs) were measured in the striatum of normal rats and in rats unilaterally lesioned with 6-OHDA after intravenous administration of saline (baseline), D_2 agonist quinpirole (1.0 mg/kg) or D_2 antagonist raclopride (6.0 mg/kg).

Results—Baseline %ID/g reached a maximum at 90 sec and maintained plateau for 3.5 min, and then declined slowly thereafter. In 6-OHDA-lesioned rats, %ID/g was significantly higher in the lesioned side compared to the intact side and the baseline total %ID/g (data from both hemispheres were combined) was significantly higher compared to quinpirole stimulation starting from 4.5 min until the end of acquisition at 30 min. Raclopride did not produce any change in uptake compared to baseline or between the hemispheres.

Conclusion—Thus, increase of A_{2A} receptor mediated uptake of radioactive **MRS5425** could be a superior molecular target for Parkinson's imaging.

[*]**Address correspondence to:** Dale O. Kiesewetter, Ph.D.; Laboratory of Molecular Imaging and Nanomedicine, National Institute of Biomedical Imaging and Bioengineering, National Institutes of Health, Bldg. 10, Room B3B25, Bethesda, MD, 20892, USA. Tel: + 1 (301) 451 3531; Fax: + 1 (301) 480 0228; dk7k@nih.gov.

Keywords

SCH442416; MRS5425; Parkinson disease; adenosine A_{2A}; 6-OHDA; rat

Introduction

The adenosine A_{2A} receptors (A_{2A}) and dopamine D_2 receptors (D_2) belong to the superfamily of rhodopsin-like G protein-coupled receptors which transduce extracellular stimuli to activate intracellular signaling pathways. These receptors exert opposite regulatory control on receptor-mediated adenylate cyclase activity at the cellular level [1]. In the brain, A_{2A} receptors are mainly expressed in the basal ganglia specifically in the striatum (caudate-putamen), nucleus accubens, and olfactory tubercle [2, 3]. Consistent with the regulatory role on adenylate cyclase activity, A_{2A} and D_2 receptors or mRNA of such receptors are co-localized on striatopallidal GABAergic neurons in the rat striatum [4, 5].

The administration of A_{2A} receptor agonists decreases the affinity of D_2 receptors [1, 6], and conversely A_{2A} receptors are antagonized by quinpirole, a D_2 receptor agonist [7]. Thus, co-localization and functionally oppositional link implicates D_2 and A_{2A} receptor interactions at the level of basal ganglia as a molecular target for pharmacotherapy in Parkinson's disease and schizophrenia [1, 8, 9]. Antagonists of A_{2A} receptors have recently emerged as a leading candidate class of non-dopaminergic anti-Parkinsonian agents, as patients undergoing dopamine replacement therapy typically experience decreased therapeutic relief as neuronal loss and symptoms inexorably progress [10].

Parkinson's disease is a progressive neurodegenerative disease that results in degeneration of pre-synaptic dopamine projections and ultimately depletion of dopamine in the basal ganglia [11, 12]. This disease has been modeled in rats by unilaterally injecting the selective monoaminergic toxin, 6-hydroxydopamine (6-OHDA), into the substantia nigra or medial forebrain bundle [13, 14], which causes neuronal death [15]. Motor deficits occur 1 week after 6-OHDA administration, which is demonstrated by animal rotation in response to the dopaminergic D_1/D_2 receptor agonist, apomorphine [16]. After 4 weeks, the animal is considered a model of late-stage asymmetrical Parkinson's disease [17].

In Parkinson's disease patients and in 6-OHDA-lesioned rats, post-synaptic D_2 receptors are upregulated [18–21], particularly in the putamen nucleus [20, 22]. A_{2A} receptor density, functionality, or mRNA of A_{2A} receptors have been reportedly increased in the caudate-putamen in Parkinson's disease patients [23, 24], Moreover, the development of a dyskinesigenic response to L-DOPA, a dopamine supplement drug which relieves some of the symptoms but does not stop Parkinson's disease progression, is correlated to post-mortem increases in A_{2A} receptor mRNA [25, 26]. In 6-OHDA-lesioned rats, mRNA of A_{2A} receptors is increased in the striatum [21]. Taken together, all these observations suggest that either D_2 receptor or A_{2A} receptor could be used as a target for molecular imaging using positron emission tomography (PET) in 6-OHDA-lesioned rats or in Parkinson's disease. D_2 receptor-mediated base line fatty acid signaling (in response to saline) is reported to be increased in 6-OHDA-lesioned rats and more so in response to quinpirole using autoradiography [27, 28]. So far, D_2 receptor-mediated PET imaging in relation to Parkinson's disease has not contributed to the benefit of patients. Thus, A_{2A} receptor mediated PET imaging can be a major contribution for early identification of Parkinson's disease, however it would only be possible if a suitable radiotracer is available. To this end two [^{11}C]ligands have been explored in human studies: [^{11}C]TMSX in normal human brain [29] and [^{11}C]SCH442416 in a study of receptor occupancy [30].

In order to take advantage of the longer half-life of fluorine-18 over carbon-11, we developed ^{18}Flabeled A_{2A} analog PET radiotracer 7-(3-(4-(2-[^{18}F]fluoroethoxy)phenyl)propyl)-2-(furan-2-yl)-7H-pyrazolo[4,3-e][1,2,4]triazolo[1,5-c]pyrimidin-5-amine ([^{18}F]-**MRS5425**), derived from SCH442416, which may allow the *in vivo* evaluation of A_{2A} receptor-mediated uptake in rat brains. The synthesis and evaluation of this novel ^{18}F-labeled compound is the subject of this manuscript. We investigated the uptake kinetics of [^{18}F]-**MRS5425** in normal rats and examined the A_{2A} receptor-mediated uptake in normal rats (without lesion) compared to unilaterally 6-OHDA-lesioned rats by using quantitative PET imaging technique. Based on evidence that ipsilateral striatum in these lesioned animals have increased A_{2A} receptor densities (*vide supra*), we predicted that the A_{2A} receptor-mediated uptake would be increased depending on the extent of A_{2A} upregulation. The ability to image D_2 and A_{2A} interaction in 6-OHDA-lesioned rats is currently unavailable, we therefore quantified region-of-interest (ROI)–derived percentage of injected dose per gram (%ID/g) in PET imaging in rats acutely administered intravenously either saline (1 mL/kg), quinpirole (a D_2, D_3 receptor agonist, 1.0 mg/kg), or raclopride (a D_2 receptor antagonist, 6 mg/kg).

Materials and Methods

General

SCH442416 (2-(furan-2-yl)-7-(3-(4-methoxyphenyl)propyl)-7*H*-pyrazolo[4,3-*e*][1,2,4]triazolo[1,5-*c*]pyrimidin-5-amine) was purchased from Tocris Biosciences (Ellisville, MO). Ethane-1,2-diol bis(3,4-dibromobenzenesulfonate (**2**), was prepared according to a literature procedure [31]. All other solvents and reagents were obtained from commercial sources and used as received. *In vitro* metabolism evaluation was conducted in cryopreserved rat hepatocytes with analysis of the generated metabolites by HPLC-MS [32]. Authentic non-radioactive MRS5425 (7-(3-(4-(2-fluoroethoxy)phenyl)propyl)-2-(furan-2-yl)-7H-pyrazolo[4,3-e][1,2,4]triazolo[1,5-c]pyrimidin-5-amine), was prepared as previously described [33].

Synthesis of phenolic precursor for radiolabeling

Commercially available SCH442416 was demethylated with boron tribromide (1M in CH_2Cl_2) at room temperature, to furnish the previously reported phenol **1** (4-(3-(5-amino-2-(furan-2-yl)-7*H*-pyrazolo[4,3-*e*][1,2,4]triazolo[1,5-*c*]pyrimidin-7-yl)propyl)phenol) in quantitative yield with characterization data identical to the published values [34]. Phenol **1** was used for radiolabeling without further purification (see Scheme 1).

Radiosynthesis of 7-(3-(4-(2-fluoroethoxy)phenyl)propyl)-2-(furan-2-yl)-7H-pyrazolo[4,3-e][1,2,4]triazolo[1,5-c]pyrimidin-5-amine (F-18 labeled fluoroethyl derivative of SCH442416, [^{18}F]-MRS5425)

Aqueous [^{18}F]fluoride (1.85 GBq, 50 mCi), 0.5 mg of potassium carbonate, and 2.3 mg K-222 were evaporated to dryness in a 10 mL glass tube under a stream of argon while heating to 105 °C. Ethane-1,2-diol bis(3,4-dibromobenzenesulfonate) (3 mg in 0.3 mL of acetonitrile) was added, the tube capped, and the resulting solution heated at 120 °C in a CEM microwave apparatus (CEM Corp, Matthews, NC, USA) for 5 min. The reaction mixture was then cooled, diluted with 0.5 mL of HPLC solvent and injected onto a Phenomenex semi-preparative C-18 HPLC column running at 5 mL/min using 50% acetonitrile in water. The desired product (2-fluoroethyl 3, 4-dibromobenzenesulfonate) was collected from HPLC at 10 min, diluted with 10 mL of water and trapped on a Waters C-18 Sep-Pak cartridge. The C-18 cartridge was washed with 10 mL of water and the radioactive product was eluted with 1 mL of dichloromethane into a 1 mL plastic tube. The small amount of water on top of organic layer was removed and the organic layer, which

contained the radioactive product, was transferred to a 10 mL glass tube. The dichloromethane was evaporated under a stream of argon gas, then 5 mg of **1**, 10 μL of 40% aqueous tetrabutylammonium hydroxide solution, and 0.3 mL of acetonitrile were added. The tube was sealed and heated at 120 °C in the microwave reactor for 5 min. After cooling, the reaction mixture was diluted with 0.5 mL of HPLC eluent and injected onto the semi-preparative reversed phase HPLC column. The HPLC column was eluted with 35% acetonitrile 65% 100 mM ammonium acetate at 5 mL/min. The desired product had a retention time of 35 min. The fraction containing the product was diluted with 15 mL of water then passed through a 100 mg C-18 column, which trapped the desired radiochemical product. The C-18 column was washed with 10 mL of water and the final product was eluted with 0.2 mL of ethanol. The total synthesis and purification time was about 130 min.

Animals

This study was conducted under a protocol approved by the Animal Care and Use Committee of the Clinical Center, National Institute of Health (NIBIB Protocol # PET 08-01). Experiments were conducted following the Guide for the Care and Use of Laboratory Animals (NIH Publication 86-23). Unilaterally 6-OHDA-lesioned male Sprague-Dawley (SD) rats were purchased from Taconic Albany (Germantown, NY, USA). In brief, at 8 weeks of age, each rat was anesthetized with sodium pentobarbital (13 mg/dL), and the left substantia nigra was lesioned by a 4-μL/min infusion of 0.1 mg/mL of 6-OHDA in 0.9% saline (w/v) at the following coordinates from the bregma: AP = −4.3, ML = +1.2, and DV = −8.3 mm.

To assess the efficacy of the 6-OHDA lesion, each lesioned rat was tested 21 days later for its response to S-(+)-apomorphine HCl (0.5 mg/kg i.p.). Only rats that completed at least 100 contralateral rotations in 20 min [28] [27] were shipped to our animal facility. Another group of SD rats without any lesion was received from the same source and was used for *in vivo* biodistribution, tissue binding studies and as controls for PET scanning.

Once received, animals were maintained in a facility that has constant temperature, humidity, and light cycles (6:00 AM – 6:00 PM), and they were given free access to food pellets (NIH-31 18-4 diet, Zeigler Bros, Gardners, PA, USA) and water. The lesioned rats were reported to have increased expression of A_{2A} receptors [35], and loss of tyrosine hydroxylase immunoreactivity in the ipsilateral basal ganglia and substantia nigra [17, 28, 36, 37]. The weight of the first group of 6-OHDA lesioned animals at time of study, ranged from 326 to 448 g. The second group ranged from 285 – 354 g. Normal rats ranged from 280 to 387 g. We did not adjust for the body weight of the animals.

In vitro binding in rat brains

Twelve-week old male SD rats (n = 4) were used for autoradiography. After sacrificing the rats by carbon dioxide asphyxiation, the brains were removed and immediately quick-frozen in dry ice. The brain was cut coronally into 20-μm slices using a Vibratome Ultrapro 5000 (Vibratome, St. Louis, MO). The slices were thaw-mounted onto adhesive coated slides, air dried for 30 min and then stored at −70° C until use. The incubation buffer consisted of 50 mM Tris at pH 7.5with 10 mM $MgCl_2$). One solution contained 2.3 MBq (62.5 μCi)/200 mL of [^{18}F]-**MRS5425**. For blocking studies, a solution of the unlabeled compound SCH442416 (250 nM) was prepared with the same buffer containing 2.3 MBq (62.5 μCi)/200 mL of [^{18}F]-**MRS5425**. The slides containing brain sections were brought to room temperature, separated into two groups, and pre-incubated in buffer solution for 10 min. One group of slides was incubated in solution of [^{18}F]-**MRS5425** and the other group was incubated in unlabeled compound plus [^{18}F]-**MRS5425** for 90 min. After incubation, the slides were washed at 4 °C with 1× PBS with 0.01% Triton X, air dried and placed on a phosphor

imaging plate with a pixel size of 25 μm (Fuji BAS-SR2025). After exposure overnight, the plates were scanned using a Fuji Bio-imaging Analysis system 5000.

In vivo blocking

Twelve-week old male SD rats (n= 4) were intravenously administered ~12.9 MBq (350 μCi)/rat of [^{18}F]-**MRS5425** in saline (200 – 300 μL total volume) and rats were killed by carbon dioxide asphyxiation at 30 min post injection. For blocking studies, two group of rats were intravenously administered either 20 μg/rat (n = 3) or 100 μg/rat (n = 3) of SCH442416 in 50 μL EtOH/saline solution immediately before [^{18}F]-**MRS5425**. After sacrificing the rats, the brains were removed and immediately quick-frozen in dry ice and cut coronally into 50-μm thick sections. The slices were thaw-mounted onto adhesive coated slides, air dried and placed on a phosphor imaging plate and processed for autoradiography as detailed in the earlier paragraph.

In vivo bio-distribution study in rats

For biodistribution studies, rats were injected intravenously ~11.1 MBq (300 μCi)/rat of [^{18}F]-**MRS5425** in saline (150 – 330 μL total volume) and killed by carbon dioxide asphyxiation at 30 (n = 4), 60 (n = 4) and 120 min (n = 6). The brain, blood and other tissues were taken from each animal and wet weighed. The radioactivity content of various tissues was counted using a gamma counter (Wallac Wizard, Turku, Finland). The uptake of the radioactivity was expressed as percentage of injected dose per gram (%ID/g).

PET studies

PET was performed using an Inveon microPET scanner (Siemens Medical Solutions). 6-OHDA lesioned 13 – 14 weeks old male SD rats (5 ± 1 weeks after lesioning, a model of late-stage asymmetrical PD) [17], and their age matched control (without lesion) were imaged. Under isoflurane (2 – 3% v/v in O_2) anesthesia, the rats were intravenously administered 8.6 ± 2.2 MBq (235 ± 75 μCi)/rat of [^{18}F]-**MRS5425** in saline (130 – 420 μL total volume), and emission scans were acquired for 30 min in list mode. Prior to administration of the radiotracers, 6-OHDA-lesioned rats were intravenously administered either saline (300 μL), D_2-like (D_2, D_3) receptor antagonist raclopride (6 mg/kg in saline) or D_2-like receptor agonist quinpirole (1 mg/kg in saline). These doses were chosen on the basis of prior neuroimaging studies in which drug-induced D_2 receptor stimulation or blocking have been reported [27, 38].

Upon completion of acquisition, images were reconstructed by a 2-dimensional ordered-subsets expectation maximum algorithm (2D OSEM), and no correction was applied for attenuation and scatter. For each scan, ROIs were manually drawn caudal to rostrally over the caudate-putamen (striatum) region on decay-corrected coronal brain images. The average radioactivity concentration within the caudate-putamen region was obtained from mean pixel values within the ROI volume. These mean values were converted to counts/mL/min using a conversion factor. Assuming a tissue density of 1 g/mL, the counts/mL/min were converted to counts/g/min and then divided by the injected dose to obtain an imaging ROI–derived percentage of injected dose per gram (%ID/g).

Statistical Analysis

Quantitative data were expressed as mean ± SEM. For bio-distribution studies, means were compared using 1-way ANOVA. For PET studies, %ID/g in the lesioned (left) vs. intact (right) sides of the brain was compared using a two tailed paired *t*-Test. The response to quinpirole or raclopride was compared to the baseline (saline) %ID/g using two tailed un-paired *t*-Test. *P* values less than 0.05 were considered statistically significant.

Results

Chemistry and Radiochemistry

MRS5425 has been previously synthesized and binding selectivity evaluated [33]. CLogP, a calculated measure of lipophilicity (ChemDraw, CambridgeSoft), was 3.18 for MRS5425 compared with 2.93 for SCH442416. The compound displays a K_i of 12.4 nM for A_{2A} with a 1000 fold selectivity over A_1 and A_3. [^{18}F]-**MRS5425** was prepared using a two-step radiosynthesis sequence (scheme 2). The intermediate [^{18}F]fluoroethyl 3,4-dibromobenzene sulfonate (**3**) was obtained by treating ethane-1,2-diol bis(3,4-dibromobenzenesulfonate (**2**) with [^{18}F]fluoride in the presence of K-222 and K_2CO_3 and heating in a microwave. Purified **3** was then reacted with the phenol **1** under basic conditions to provide [^{18}F]-**MRS5425**, which was purified by HPLC and formulated for injection. The radiochemical yield based on starting [^{18}F]fluoride and uncorrected for decay was 14.5 ± 3.6% (n = 8). The radiochemical purity was greater than 98%.

In Vitro Brain autoradiography

Figure 1 (a– f) presents the representative distribution of radioactivity on coronal rat brain slices by the phosphor-imaging technique. Brain slices incubated with [^{18}F]-**MRS5425** for 90 min showed radioactivity binding (dark area in Fig 1 b) in the caudate-putamen (striatum) nucleus bilaterally. This binding to adenosineA_{2A} was receptor specific as it could be blocked by co-incubation with non-radioactive adenosine A_{2A} antagonist SCH442416 (Fig 1 c).

Ex vivo Brain autoradiography

In the rats sacrificed at 30 min after [^{18}F]-**MRS5425** injection, 50 μm thick brain slices showed radioactivity binding in the striatal region bilaterally (Fig. 1d). This *ex vivo* striatal binding was selective and could also be dose dependently blocked by pre-administration of non-radioactive A_{2A} antagonist. When the rats were intravenously administered SCH442416 (20 μg/rat or 100 μg/rat) immediately prior to [^{18}F]-**MRS5425**, striatal binding was slightly reduced at 20 μg/rat (Fig 1 e), and more so at 100 μg/rat (Fig 1f).

In vivo biodistribution

In order to evaluate the kinetics of uptake and selective tissue accumulation, we conducted *in vivo* biodistribution studies after intravenous administration of [^{18}F]-**MRS5425** in rats. The animals were killed at 30, 60, and 120 min, and various tissues were harvested for gamma counting and the data reported as % ID/g (Fig 2). The uptake in the A_{2A} receptor-containing striatum was 0.25 ± 0.09 %ID/g at 30 min (n = 4) and 0.35 ± 0.10 %ID/g at 60 min (n = 4) after injection followed by a significant reduction to 0.13 ± 0.03%ID/g at 120 min (n = 6). The biodistribution studies showed the primary accumulation to be in the intestine and urine, through the metabolism of liver and kidneys, respectively.

PET kinetic experiment in normal rats

The radioactivity signal displayed in pseudo color-coded images in Figure 3a, showed that the striatum (red and yellow) had significantly higher uptake than the cortical and other regions (blue). The time activity curve (TAC) for [^{18}F]-**MRS5425** measured in the striatum of rat brain is shown in Fig. 4a. The imaging ROI–derived %ID/g reached a maximum at 90 sec and maintained a plateau for 2 additional minutes. Then %ID/g declined slowly to 75% of peak value at about 6 min and 50% of peak uptake by 17 min. The TAC measured in the striatum was significantly higher from the cortex or cerebellum (data not shown).

PET kinetic experiment in 6-OHDA-lesioned rats

The radioactivity signal displayed in pseudo color-coded images showed that the striatum (red and yellow) in the lesioned side (arrow) is higher than the intact side (Fig. 3b). When unilaterally 6-OHDA-lesioned rats were administered saline before [^{18}F]-**MRS5425**, the baseline %ID/g in the striatum of both lesioned and intact sides peaked at 90 sec, as in the normal rats, and maintained a brief plateau for about 3 min, which is one minute prolonged compared to normal rats (Fig. 4 a and b). From that time point to the end of acquisition at 30 min, TAC showed that %ID/g is significantly higher in the lesioned side compared to intact side ($p < 0.05$).

When unilaterally 6-OHDA-lesioned rats are administered D_2 receptor agonist quinpirole or D_2 receptor blocker raclopride before [^{18}F]-**MRS5425**, there is no difference in %ID/g in the striatum between lesioned and intact sides (data not shown). Data from both hemispheres, therefore, were combined and referred to as “total %ID/g” data. The total %ID/g response to either quinpirole or raclopride was compared to baseline (total %ID/g response to saline). TAC showed that the baseline total %ID/g is significantly higher compared to quinpirole stimulation starting from 4.5 min until the end of acquisition at 30 min (Fig. 4c). There is no difference in total %ID/g response in rats between saline and raclopride (data not shown).

Discussion

MRS5425 is a high affinity A_{2A} ligand with 1000-fold selectivity over other adenosine receptor subtypes. Although somewhat lower affinity than SCH442416, the affinity data predict good imaging results. There is very little difference between MRS5425 and SCH442416 in calculated cLogP. We demonstrated specific uptake using ex vivo autoradiography, which showed that uptake of [^{18}F]MRS5425 was significantly (20 ug) or completely (100 ug) reduced by pre-administration of SCH442416 (Figure 1d–1f). By studying [^{18}F]-**MRS5425** binding, kinetics and TAC in the rat brain at baseline (saline) and in response to quinpirole and raclopride, we have separated the radioactive uptake arising from adenosine A_{2A} receptors in normal rats and in a rat model of unilateral PD. Our choice of these drugs for competition studies with [^{18}F]-MRS5425 were hypothesis driven based on the anticipated effect on the radioligand uptake.

We elected to use the hemi-Parkinson’s rat model, which would allow the non-lesioned side as an internal control. The hemi-Parkinson’s model is created by 6-hydroxydopamine injection into the area of substantia nigra or medial forebrain bundle. The neurotoxin causes a reduction of dopamine signaling in the striatum. The model is commercially available and the literature reports of the stereotaxic coordinates for the injection vary somewhat. The model is verified by the characteristic rotation pattern of the lesioned rats following treatment with apomorphine. Rats subjected to unilateral lesion of the substantia nigra at 8 weeks of age, and studied while anesthetized at 13–14 weeks of age, demonstrated significantly increased values of %ID/g of [^{18}F]MRS5425, a marker of adenosine A_{2A} receptor-mediated uptake, in the striatum on the lesioned compared with intact hemisphere. An unpaired t-test analysis showed that 1 mg/kg i.v. of quinpirole, a D_2 receptor agonist, produced a statistically significant decrease in total %ID/g (measured in bilateral striatum) compared with baseline (total %ID/g response to saline) in 6-OHDA-lesioned rats. In contrast to quinpirole, 6 mg/kg i.v. of raclopride, a D_2 receptor antagonist did not produce any significant change in total %ID/g compared with saline.

A biodistribution study has been reported in normal rats after injecting [^{11}C]-SCH442416, the maximum radioactivity accumulation measured in the striatum was at 5 min [39] and thereafter %ID/g declined rapidly and reached 50% of its peak by 25 min and to its lowest

value by 60 min. In the study presented here, %ID/g measured in the striatum in normal rats at 30 min and 60 min are almost at the same level and declined thereafter. Blood may continue to provide input function over 2 h (see Fig. 2), however, parent compound in the blood was not determined in our study. In spite of the blood-brain-barrier, uptake of [^{18}F]-**MRS5425** in the striatum was ~ 2-fold higher at 30 and 60 min compared to blood. This suggests that [^{18}F]-**MRS5425** may be a viable molecular imaging probe for pathological conditions with elevated adenosine A_{2A} receptors.

We analyzed by HPLC-MS *in vitro* rat hepatocyte metabolism of [^{18}F]MRS5425 and observed a major fluorine-containing metabolite, which because of its significantly higher polarity and the increase in the m/z by 16 was believed to be the result of N-oxidation. This compound would not be expected to cross the blood-brain barrier. There was also evidence for defluorination in the rat hepatocyte incubation. Defluorination, manifested by skull uptake can confound accurate quantitation in brain cortex [40]. However, bone uptake was not observed in our imaging studies, which indicates that this is an insignificant metabolite in rats.

Our results are comparable to a previous PET study using [^{11}C]-SCH442416 in anesthetized monkeys [39]. In that study, the greatest radioactivity of [^{11}C]-SCH442416 was detected at the striatum, and lower levels were found in the cerebellum and cortex. Consistent with that report, we also observed low values of %ID/g in those areas compared to striatum. The concentration of A_{2A} receptors are negligible in the cerebellum and cortical brain regions [6] and thus, would contribute to low values of %ID/g. In the study presented here, the %ID/g measured in the striatum peaked at 90 sec after administering [^{18}F]-**MRS5425**, held a plateau until 3.5 min in normal rats and 4.5 min in 6-OHDA rats, and declined slowly thereafter. Due to huge species differences in blood flow and metabolism, the %ID/g values that we observed are about ~20-fold greater, and had peaked earlier compared with 0.035 %ID/mL measured (between 2 min and 4 min acquisition frame) in monkeys using [^{11}C]-SCH442416 [39].

In PET imaging, the higher baseline ipsilateral values of %ID/g (following saline) in 6-OHDA-lesioned rats was coherent with our early prediction. They likely represented upregulated or disinhibited baseline A_{2A} receptor-mediated uptake in ipsilateral extrapyramidal and related circuitry, due to increased sensitivity to A_{2A} analog in relation to increased levels of A_{2A} receptors [21, 23, 24, 26, 41]. In addition to direct A_{2A} receptor mediated uptake, the increased baseline values of %ID/g could have reflected increased A_{2A} signaling *via* stimulatory metabotropic glutamate mGlu5 receptors [42] or via activating other adenylate cyclase-coupled neuroreceptors including D_2. As 6-OHDA-lesioning also upregulates the post-synaptic D_2 receptors [18, 26, 43] and removes the D_2 inhibition at the level of the A_{2A} activated adenylate cyclase, the result is an enhancement of A_{2A} receptor-mediated uptake [44–46]. Rats lesioned with 6-OHDA have a 20% increase in mRNA, protein, and/or transcription of A_{2A} receptors [21]; a 30–280% increase in these markers of A_{2A} have been observed in Parkinson's disease patients [23, 24]. We found a statistically significant increase of 9~ 12% in the %ID/g in the lesioned striatum, which is consistent with the upregulation of A_{2A} receptors in rats. If a similar trend is translated in human, A_{2A} receptor-mediated PET imaging could be a crucial tool to identify human Parkinson's disease.

In normal brain, A_{2A} receptor is oppositionally coupled with the D_2 receptors at the striatopallidal neurons [1, 6, 7]. The new finding of increased ipsilateral A_{2A}-initiated signaling and earlier evidence of increased ipsilateral D_2-initiated signaling [27, 28, 41] argue that both of the receptors became upregulated and supersensitive in the unilaterally 6-OHDA-lesioned rat model of Parkinson's disease. However, at the signaling level,

stimulation of D_2 receptors by quinpirole antagonizes the effects secondary to A_{2A} receptor mediated signaling [7, 44, 47]. In agreement, we identified that A_{2A}-mediated total %ID/g response was significantly decreased after acute injection of quinpirole. However, we did not find asymmetry in A_{2A}-mediated uptake in response to either quinpirole or raclopride in unilaterally 6-OHDA-lesioned rats, which is further to be explored.

In summary, A_{2A} receptor mediated uptake was increased in the striatum ipsilateral to a 6-OHDA-lesioned rats, a model of late stage asymmetrical Parkinson's disease. This increase corresponds to reported elevated expression of A_{2A} receptors in the regions and could be an imperious molecular target for Parkinson's imaging. An upregulated A_{2A} initiated signaling associated with D_2 receptor supersensitivity may exist in Parkinson's disease and contribute to its symptoms.

Acknowledgments

This research was supported by the Intramural Research Program of the National Institute of Biomedical Imaging and Bioengineering (NIBIB) and the National Institute of Diabetes and Digestive and Kidney Diseases (NIDDK).

References

1. Ferre S, Fredholm BB, Morelli M, Popoli P, Fuxe K. Adenosine-dopamine receptor-receptor interactions as an integrative mechanism in the basal ganglia. Trends in neurosciences. 1997; 20:482–487. [PubMed: 9347617]
2. Ongini E, Fredholm BB. Pharmacology of adenosine A2A receptors. Trends in pharmacological sciences. 1996; 17:364–372. [PubMed: 8979771]
3. Cunha RA, Johansson B, van der Ploeg I, Sebastiao AM, Ribeiro JA, Fredholm BB. Evidence for functionally important adenosine A2a receptors in the rat hippocampus. Brain research. 1994; 649:208–216. [PubMed: 7953635]
4. Fink JS, Weaver DR, Rivkees SA, Peterfreund RA, Pollack AE, Adler EM, et al. Molecular cloning of the rat A2 adenosine receptor: selective co-expression with D2 dopamine receptors in rat striatum. Brain Res Mol Brain Res. 1992; 14:186–195. [PubMed: 1279342]
5. Schiffmann SN, Jacobs O, Vanderhaeghen JJ. Striatal restricted adenosine A2 receptor (RDC8) is expressed by enkephalin but not by substance P neurons: an in situ hybridization histochemistry study. Journal of neurochemistry. 1991; 57:1062–1067. [PubMed: 1713612]
6. Svenningsson P, Le Moine C, Fisone G, Fredholm BB. Distribution, biochemistry and function of striatal adenosine A2A receptors. Progress in neurobiology. 1999; 59:355–396. [PubMed: 10501634]
7. Vortherms TA, Watts VJ. Sensitization of neuronal A2A adenosine receptors after persistent D2 dopamine receptor activation. The Journal of pharmacology and experimental therapeutics. 2004; 308:221–227. [PubMed: 14566008]
8. Aoyama S, Kase H, Borrelli E. Rescue of locomotor impairment in dopamine D2 receptor-deficient mice by an adenosine A2A receptor antagonist. J Neurosci. 2000; 20:5848–5852. [PubMed: 10908627]
9. Fredduzzi S, Moratalla R, Monopoli A, Cuellar B, Xu K, Ongini E, et al. Persistent behavioral sensitization to chronic L-DOPA requires A2A adenosine receptors. J Neurosci. 2002; 22:1054–1062. [PubMed: 11826134]
10. Schwarzschild MA, Agnati L, Fuxe K, Chen JF, Morelli M. Targeting adenosine A2A receptors in Parkinson's disease. Trends in neurosciences. 2006; 29:647–654. [PubMed: 17030429]
11. Hornykiewicz O. Imbalance of brain monoamines and clinical disorders. Prog Brain Res. 1982; 55:419–429. [PubMed: 7163495]
12. Heiss WD, Hilker R. The sensitivity of 18-fluorodopa positron emission tomography and magnetic resonance imaging in Parkinson's disease. Eur J Neurol. 2004; 11:5–12. [PubMed: 14692881]

13. Gerlach M, Riederer P. Animal models of Parkinson's disease: an empirical comparison with the phenomenology of the disease in man. J Neural Transm. 1996; 103:987–1041. [PubMed: 9013391]
14. Ungerstedt U. Postsynaptic supersensitivity after 6-hydroxy-dopamine induced degeneration of the nigro-striatal dopamine system. Acta Physiol Scand Suppl. 1971; 367:69–93. [PubMed: 4332693]
15. Jeon BS, Jackson-Lewis V, Burke RE. 6-Hydroxydopamine lesion of the rat substantia nigra: time course and morphology of cell death. Neurodegeneration. 1995; 4:131–137. [PubMed: 7583676]
16. Arnt J, Hyttel J. Differential involvement of dopamine D-1 and D-2 receptors in the circling behaviour induced by apomorphine, SK & F 38393, pergolide and LY 171555 in 6-hydroxydopamine-lesioned rats. Psychopharmacology. 1985; 85:346–352. [PubMed: 2860689]
17. Yuan H, Sarre S, Ebinger G, Michotte Y. Histological, behavioural and neurochemical evaluation of medial forebrain bundle and striatal 6-OHDA lesions as rat models of Parkinson's disease. J Neurosci Methods. 2005; 144:35–45. [PubMed: 15848237]
18. Cadet JL, Zhu SM. The intrastriatal 6-hydroxydopamine model of hemiparkinsonism: quantitative receptor autoradiographic evidence of correlation between circling behavior and presynaptic as well as postsynaptic nigrostriatal markers in the rat. Brain research. 1992; 595:316–326. [PubMed: 1467973]
19. Chalon S, Emond P, Bodard S, Vilar MP, Thiercelin C, Besnard JC, et al. Time course of changes in striatal dopamine transporters and D2 receptors with specific iodinated markers in a rat model of Parkinson's disease. Synapse (New York, N.Y. 1999; 31:134–139.
20. Ichise M, Kim YJ, Ballinger JR, Vines D, Erami SS, Tanaka F, et al. SPECT imaging of pre- and postsynaptic dopaminergic alterations in L-dopa-untreated PD. Neurology. 1999; 52:1206–1214. [PubMed: 10214745]
21. Pinna A, Corsi C, Carta AR, Valentini V, Pedata F, Morelli M. Modification of adenosine extracellular levels and adenosine A(2A) receptor mRNA by dopamine denervation. European journal of pharmacology. 2002; 446:75–82. [PubMed: 12098587]
22. Antonini A, Vontobel P, Psylla M, Gunther I, Maguire PR, Missimer J, et al. Complementary positron emission tomographic studies of the striatal dopaminergic system in Parkinson's disease. Arch Neurol. 1995; 52:1183–1190. [PubMed: 7492293]
23. Hurley MJ, Mash DC, Jenner P. Adenosine A(2A) receptor mRNA expression in Parkinson's disease. Neuroscience letters. 2000; 291:54–58. [PubMed: 10962152]
24. Varani K, Vincenzi F, Tosi A, Gessi S, Casetta I, Granieri G, et al. A2A adenosine receptor overexpression and functionality, as well as TNF-alpha levels, correlate with motor symptoms in Parkinson's disease. Faseb J. 24:587–598. [PubMed: 19776336]
25. Lang AE, Lozano AM. Parkinson's disease. Second of two parts. N Engl J Med. 1998; 339:1130–1143. [PubMed: 9770561]
26. Calon F, Dridi M, Hornykiewicz O, Bedard PJ, Rajput AH, Di Paolo T. Increased adenosine A2A receptors in the brain of Parkinson's disease patients with dyskinesias. Brain. 2004; 127:1075–1084. [PubMed: 15033896]
27. Bhattacharjee AK, Meister LM, Chang L, Bazinet RP, White L, Rapoport SI. In vivo imaging of disturbed pre- and post-synaptic dopaminergic signaling via arachidonic acid in a rat model of Parkinson's disease. Neuroimage. 2007; 37:1112–1121. [PubMed: 17681816]
28. Hayakawa T, Chang MC, Rapoport SI, Appel NM. Selective dopamine receptor stimulation differentially affects [3H]arachidonic acid incorporation, a surrogate marker for phospholipase A2-mediated neurotransmitter signal transduction, in a rodent model of Parkinson's disease. The Journal of pharmacology and experimental therapeutics. 2001; 296:1074–1084. [PubMed: 11181943]
29. Mishina M, Ishiwata K, Kimura Y, Naganawa M, Oda K, Kobayashi S, et al. Evaluation of distribution of adenosine A(2A) receptors in normal human brain measured with [C-11]TMSX PET. Synapse (New York, N.Y. 2007; 61:778–784.
30. Brooks DJ, Papapetropoulos S, Vandenhende F, Tomic D, He P, Coppell A, et al. An Open-Label, Positron Emission Tomography Study to Assess Adenosine A(2A) Brain Receptor Occupancy of Vipadenant (BIIB014) at Steady-State Levels in Healthy Male Volunteers. Clinical Neuropharmacology. 2010; 33:55–60. [PubMed: 20375654]

31. Musachio JL, Shah J, Pike VW. Radiosyntheses and reactivities of novel [F-18]2-fluoroethyl arylsulfonates. J. Label. Compd. Radiopharm. 2005; 48:735–747.
32. Ma Y, Kiesewetter D, Lang L, Eckelman WC. Application of LC-MS to the analysis of new radiopharmaceuticals. Mol Imaging Biol. 2003; 5:397–403. [PubMed: 14667494]
33. Shinkre BA, Kumar TS, Gao ZG, Deflorian F, Jacobson KA, Trenkle WC. Synthesis and evaluation of 1,2,4-triazolo[1,5-c]pyrimidine derivatives as A(2A) receptor-selective antagonists. Bioorganic & Medicinal Chemistry Letters. 2010; 20:5690–5694. [PubMed: 20801028]
34. Baraldi PG, Cacciari B, Spalluto G, Bergonzoni M, Dionisotti S, Ongini E, et al. Design, synthesis, and biological evaluation of a second generation of pyrazolo[4,3-e]-1,2,4-triazolo[1,5-c]pyrimidines as potent and selective A(2A) adenosine receptor antagonists. Journal of Medicinal Chemistry. 1998; 41:2126–2133. [PubMed: 9622554]
35. Inaji M, Okauchi T, Ando K, Maeda J, Nagai Y, Yoshizaki T, et al. Correlation between quantitative imaging and behavior in unilaterally 6-OHDA-lesioned rats. Brain research. 2005; 1064:136–145. [PubMed: 16298352]
36. Sauer H, Oertel WH. Progressive degeneration of nigrostriatal dopamine neurons following intrastriatal terminal lesions with 6-hydroxydopamine: a combined retrograde tracing and immunocytochemical study in the rat. Neuroscience. 1994; 59:401–415. [PubMed: 7516500]
37. Zuch CL, Nordstroem VK, Briedrick LA, Hoernig GR, Granholm AC, Bickford PC. Time course of degenerative alterations in nigral dopaminergic neurons following a 6-hydroxydopamine lesion. J Comp Neurol. 2000; 427:440–454. [PubMed: 11054705]
38. Bhattacharjee AK, Chang L, White L, Bazinet RP, Rapoport SI. Imaging apomorphine stimulation of brain arachidonic acid signaling via D2-like receptors in unanesthetized rats. Psychopharmacology. 2008; 197:557–566. [PubMed: 18274730]
39. Moresco RM, Todde S, Belloli S, Simonelli P, Panzacchi A, Rigamonti M, et al. In vivo imaging of adenosine A2A receptors in rat and primate brain using [11C]SCH442416. European journal of nuclear medicine and molecular imaging. 2005; 32:405–413. [PubMed: 15549298]
40. Carson RE, Wu YJ, Lang LX, Ma Y, Der MG, Herscovitch P, et al. Brain uptake of the acid metabolites of F-18-labeled WAY 100635 analogs. J. Cereb. Blood Flow Metab. 2003; 23:249–260. [PubMed: 12571456]
41. Tomiyama M, Kimura T, Maeda T, Tanaka H, Kannari K, Baba M. Upregulation of striatal adenosine A2A receptor mRNA in 6-hydroxydopamine-lesioned rats intermittently treated with L-DOPA. Synapse (New York, N.Y. 2004; 52:218–222.
42. Ferre S, Karcz-Kubicha M, Hope BT, Popoli P, Burgueno J, Gutierrez MA, et al. Synergistic interaction between adenosine A2A and glutamate mGlu5 receptors: implications for striatal neuronal function. Proceedings of the National Academy of Sciences of the United States of America. 2002; 99:11940–11945. [PubMed: 12189203]
43. Nikolaus S, Larisch R, Beu M, Forutan F, Vosberg H, Muller-Gartner HW. Bilateral increase in striatal dopamine D2 receptor density in the 6-hydroxydopamine-lesioned rat: a serial in vivo investigation with small animal PET. European journal of nuclear medicine and molecular imaging. 2003; 30:390–395. [PubMed: 12634967]
44. Kull B, Ferre S, Arslan G, Svenningsson P, Fuxe K, Owman C, et al. Reciprocal interactions between adenosine A2A and dopamine D2 receptors in Chinese hamster ovary cells co-transfected with the two receptors. Biochemical pharmacology. 1999; 58:1035–1045. [PubMed: 10509756]
45. Fuxe K, Stromberg I, Popoli P, Rimondini-Giorgini R, Torvinen M, Ogren SO, et al. Adenosine receptors and Parkinson's disease. Relevance of antagonistic adenosine and dopamine receptor interactions in the striatum. Advances in neurology. 2001; 86:345–353. [PubMed: 11553995]
46. Ferre S, Popoli P, Gimenez-Llort L, Rimondini R, Muller CE, Stromberg I, et al. Adenosine/dopamine interaction: implications for the treatment of Parkinson's disease. Parkinsonism & related disorders. 2001; 7:235–241. [PubMed: 11331192]
47. Hillion J, Canals M, Torvinen M, Casado V, Scott R, Terasmaa A, et al. Coaggregation, cointernalization, and codesensitization of adenosine A2A receptors and dopamine D2 receptors. The Journal of biological chemistry. 2002; 277:18091–18097. [PubMed: 11872740]

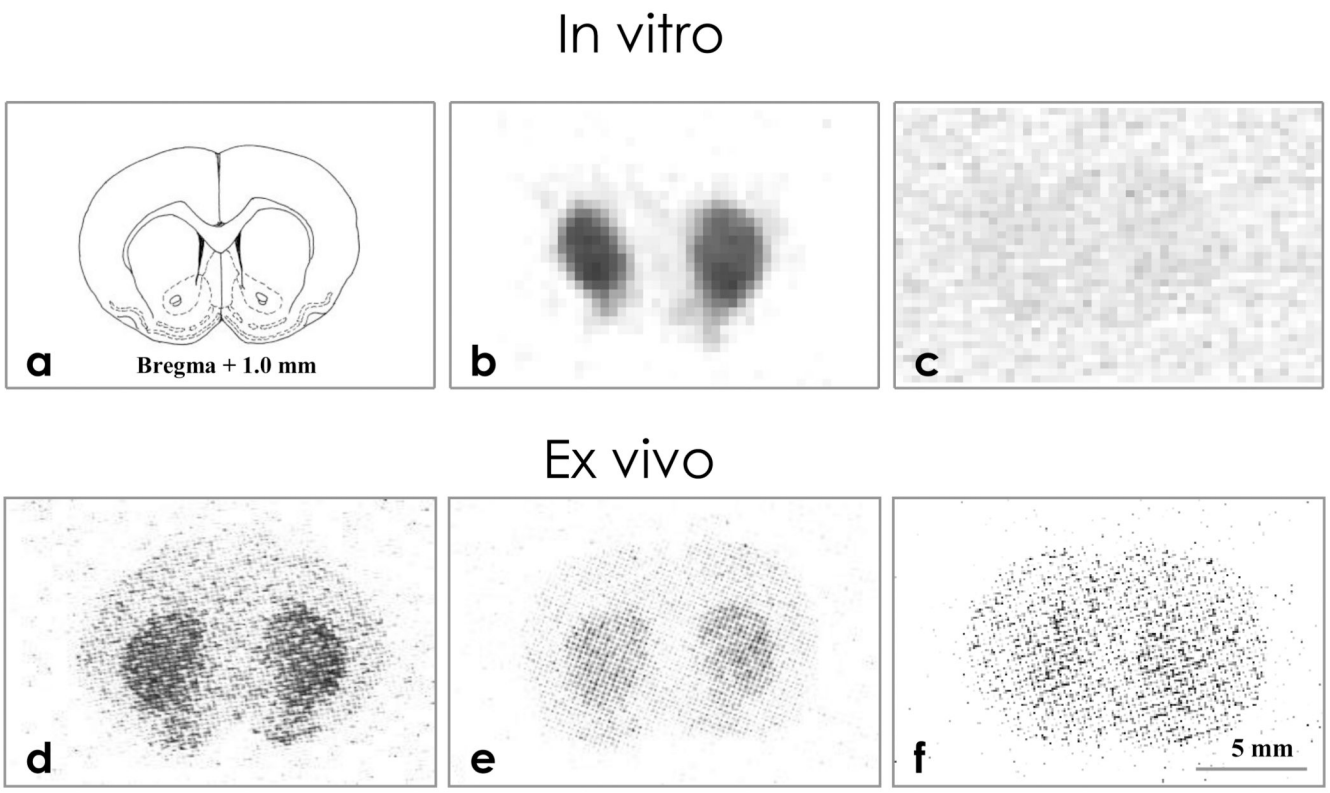

Figure 1.

In vitro and *ex vivo* autoradiography of coronal rat brain sections compared with drawing of brain anatomy (1a). *In vitro* autoradiograms following 90 min incubation with 2.3 MBq [^{18}F]-MRS5425 (1b) and co-incubation with 2.3 MBq [^{18}F]-MRS5425 and SCH442416 (1c). *Ex vivo* autoradiograms of brain slices obtained 30 min following injection of 12.9 MBq [^{18}F]-MRS5425 (1d), at the same time point following pre-administration of SCH442416 at doses of 20 μg/rat (1e) and 100 μg/rat (1f).

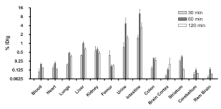

Figure 2.
In vivo biodistribution of [^{18}F]-MRS5425 (11.1 MBq dose) at 30, 60 and 120 min post-administration in normal rats.

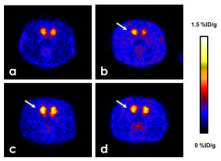

Figure 3.

PET images following administration of [^{18}F]-MRS5425 (8.6 ± 2.2 MBq). Each image is the sum of 10 min counting as indicated below the panels from left to right: (a) images in a normal rat; (b) images from a 6-OHDA-lesioned rat; (c) images from an unilaterally 6-OHDA-lesioned rat with an immediate pre-administration of quinpirole; (d) images from an unilaterally 6-OHDA-lesioned rat with a pre-administration of raclopride. The arrows in b–d indicate the 6-OHDA-lesioned side.

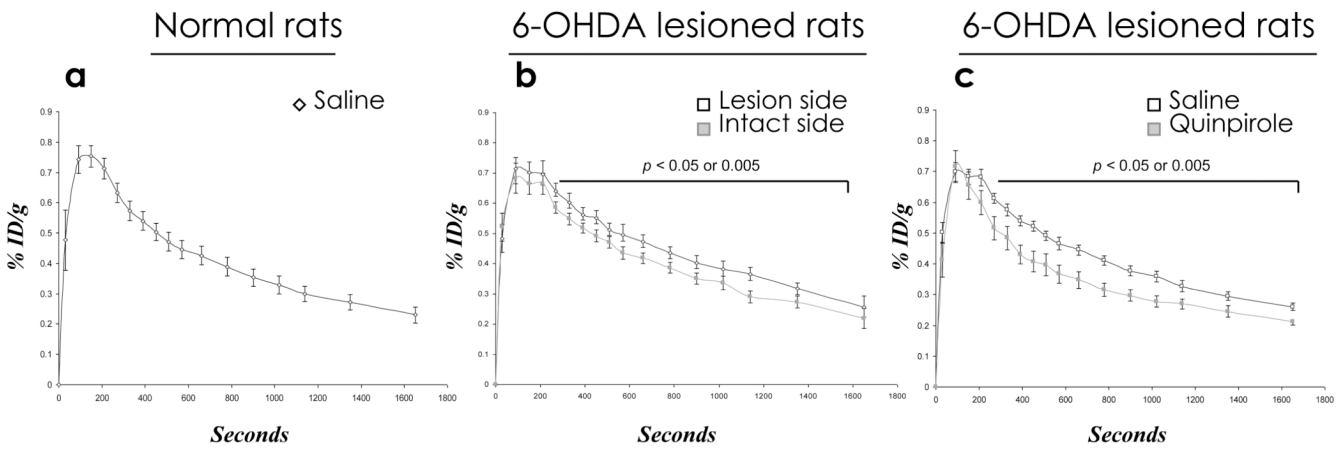

Figure 4.

Striatal time-activity-curves (TACs) determined from dynamic acquisition of PET data. a) TAC in normal rat. b) TACs for 6-OHDA-lesioned rats comparing lesioned side with intact side. $p<0.05$ at each time point beginning at 330 sec until end of scan. c) TACs for 6-OHDA-lesioned rats immediately pre-injected with saline compared with quinpirole ($p < 0.05$ from 330 sec until end of scan).

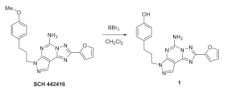

Scheme 1.

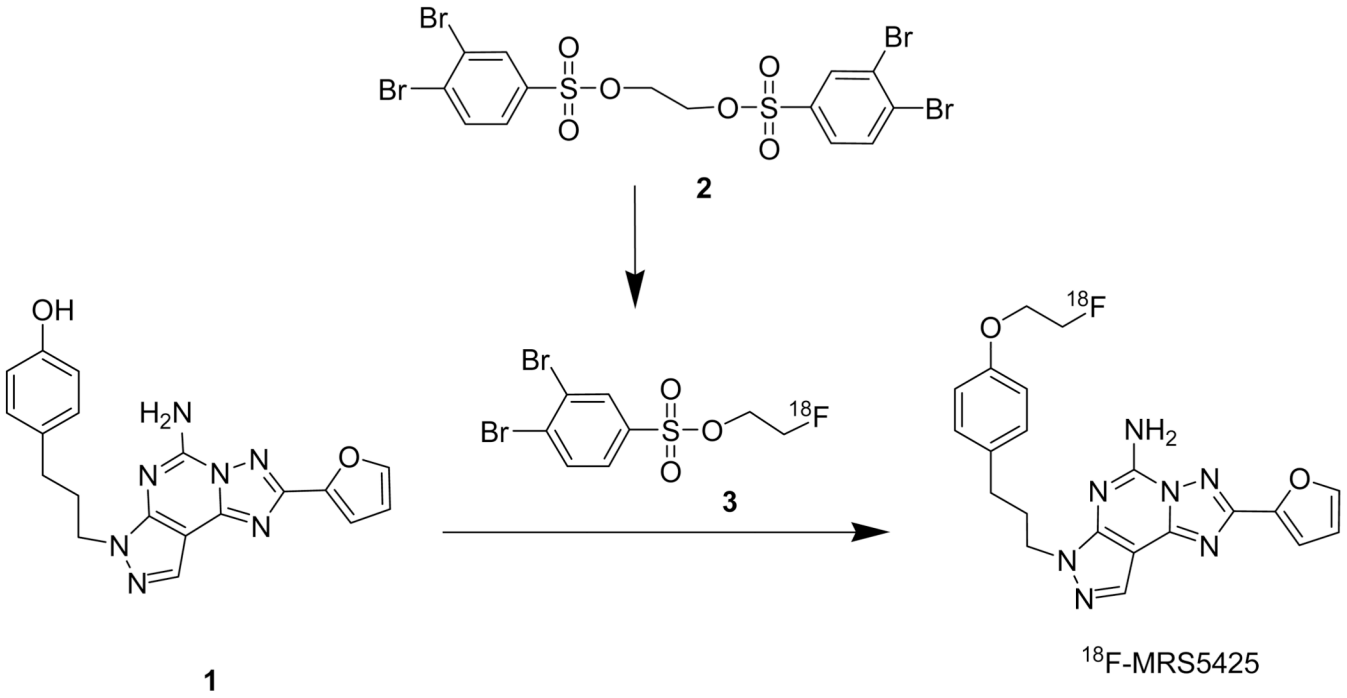

Scheme 2.
The radiochemical synthesis of [^{18}F]-**MRS5425**.